

Desymmetrizing heteroleptic [Cu(P[^]P)(N[^]N)][PF₆] compounds: effects on structural, dynamic and photophysical properties

Marco Meyer, Fabian Brunner, Alessandro Prescimone, Edwin C. Constable and Catherine E. Housecroft*

Department of Chemistry, University of Basel, BPR 1096, Mattenstrasse 24a, CH-4058 Basel, Switzerland

Table of contents

Figure S1. HMQC spectrum of **2**.

Figure S2. HMBC spectrum of **2**.

Figure S3. HMQC spectrum of **3**.

Figure S4. HMBC spectrum of **3**.

Figure S5. ORTEP representation of the structure of the [Cu(xantphos)(**3**)]⁺ cation.

Figure S6. π -Stacking interaction in the [Cu(xantphos)(**3**)]⁺ cation.

Figure S7. ¹H NMR spectrum of [Cu(POP)(**1**)]PF₆.

Figure S8. HMQC spectrum of [Cu(POP)(**1**)]PF₆.

Figure S9. HMBC spectrum of [Cu(POP)(**1**)]PF₆.

Figure S10. Part of the ¹H NMR spectrum of [Cu(xantphos)(**1**)]PF₆.

Figure S11. Part of the HMQC spectrum of [Cu(xantphos)(**1**)]PF₆.

Figure S12. Part of the HMBC spectrum of [Cu(xantphos)(**1**)]PF₆.

Figure S13. Aromatic region of the ¹H NMR spectrum of [Cu(POP)(**2**)]PF₆.

Figure S14. Aromatic region of the HMQC spectrum of [Cu(POP)(**2**)]PF₆,

Figure S15. Aromatic region of the HMBC spectrum of [Cu(POP)(**2**)]PF₆

Figure S16. Aromatic region of the ¹H NMR spectrum of [Cu(xantphos)(**2**)]PF₆.

Figure S17. Aromatic region of the HMQC spectrum of [Cu(xantphos)(**2**)]PF₆.

Figure S18. Aromatic region of the HMBC spectrum of [Cu(xantphos)(**2**)]PF₆.

Figure S19. Aromatic region of the ¹H NMR spectrum of [Cu(xantphos)(**3**)]PF₆.

Figure S20. Aromatic region of the HMQC spectrum of [Cu(xantphos)(**3**)]PF₆.

Figure S21. Aromatic region of the HMBC spectrum of [Cu(xantphos)(**3**)]PF₆.

Figure S22. Aromatic regions of the ¹H NMR spectra of [Cu(POP)(**2**)]PF₆ and [Cu(xantphos)(**2**)]PF₆.

Figure S23. Part of the NOESY spectra of [Cu(xantphos)(**2**)]PF₆ and [Cu(POP)(**2**)]PF₆.

Figure S24. Cyclic voltammograms of [Cu(POP)(**2**)]PF₆ and [Cu(xantphos)(**2**)]PF₆.

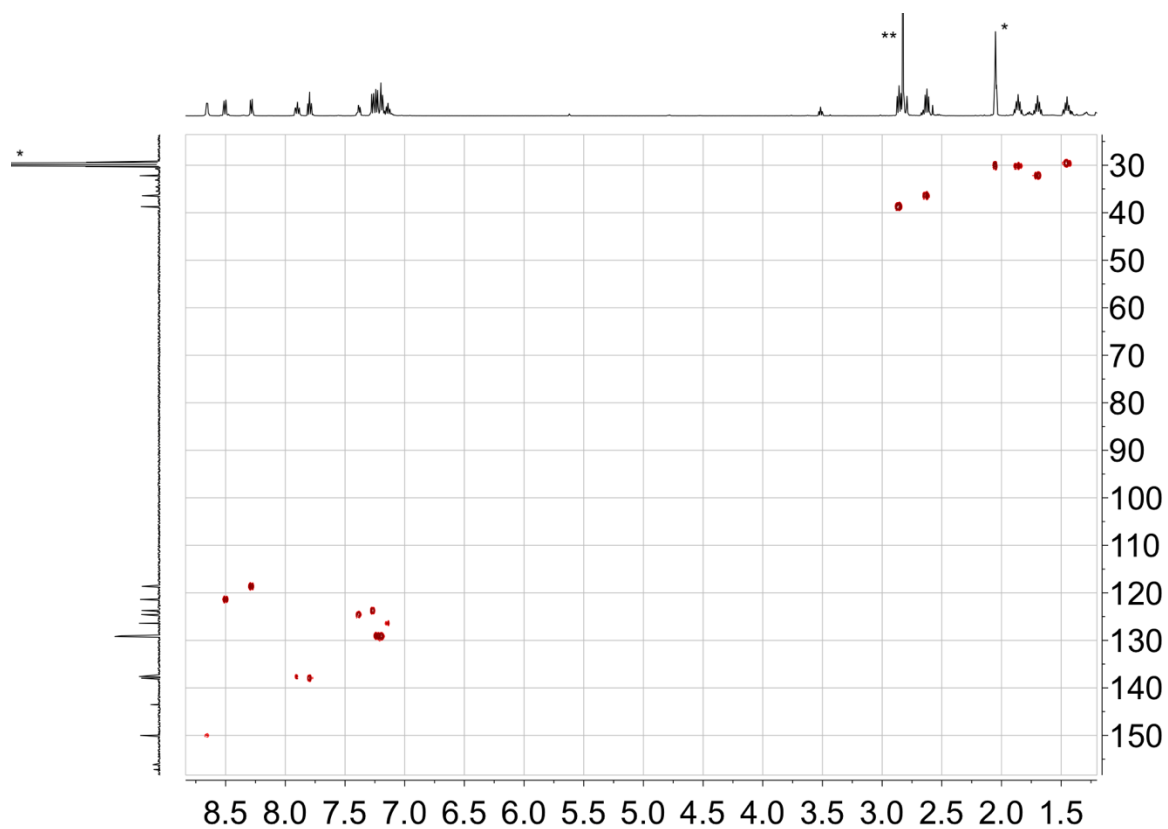


Figure S1. HMBC spectrum of **2** (^1H 500 MHz, ^{13}C 126 MHz, acetone- d_6 , 298 K). * = acetone- d_6 (in $^{13}\text{C}\{^1\text{H}\}$) or residual acetone- d_5 (in ^1H); ** = H_2O .

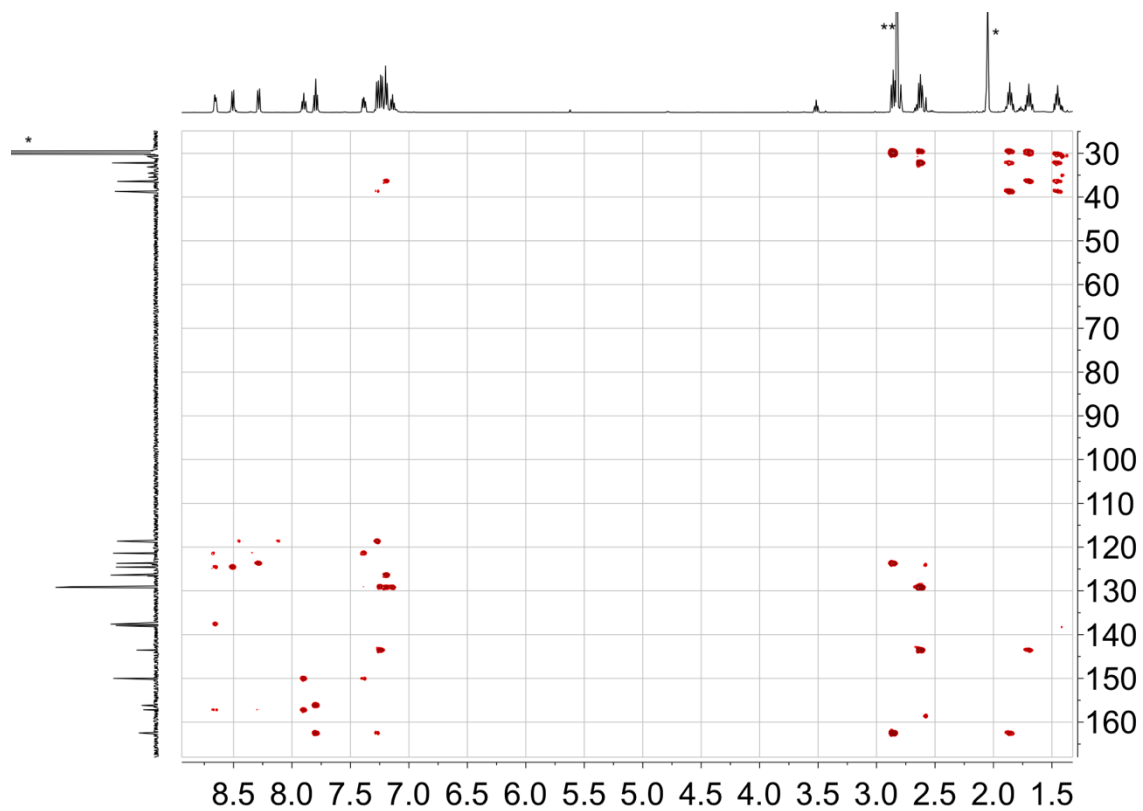


Figure S2. HMBC spectrum of **2** (^1H 500 MHz, ^{13}C 126 MHz, acetone- d_6 , 298 K). * = acetone- d_6 (in $^{13}\text{C}\{^1\text{H}\}$) or residual acetone- d_5 (in ^1H); ** = H_2O .

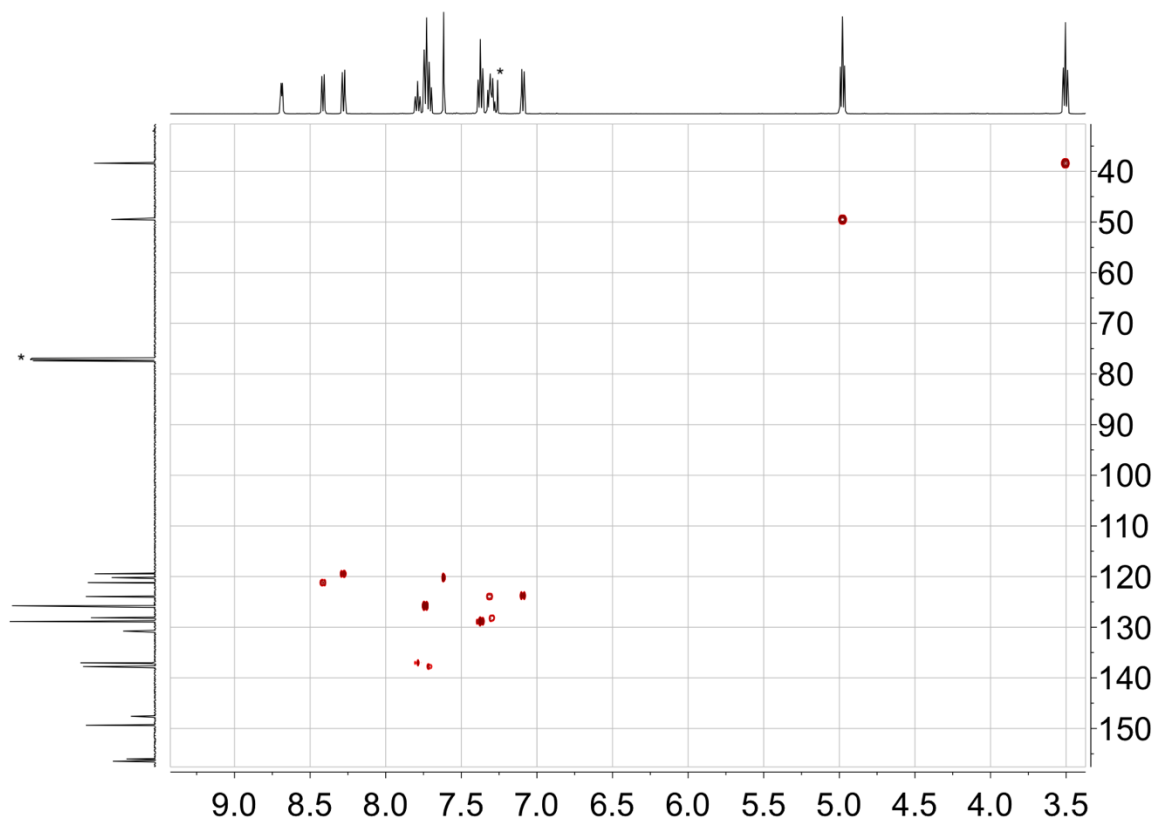


Figure S3. HMOC spectrum of **3** (^1H 500 MHz, ^{13}C 126 MHz, CDCl_3 , 298 K). * = CDCl_3 (in $^{13}\text{C}\{^1\text{H}\}$) or residual CHCl_3 (in ^1H); ** = H_2O .

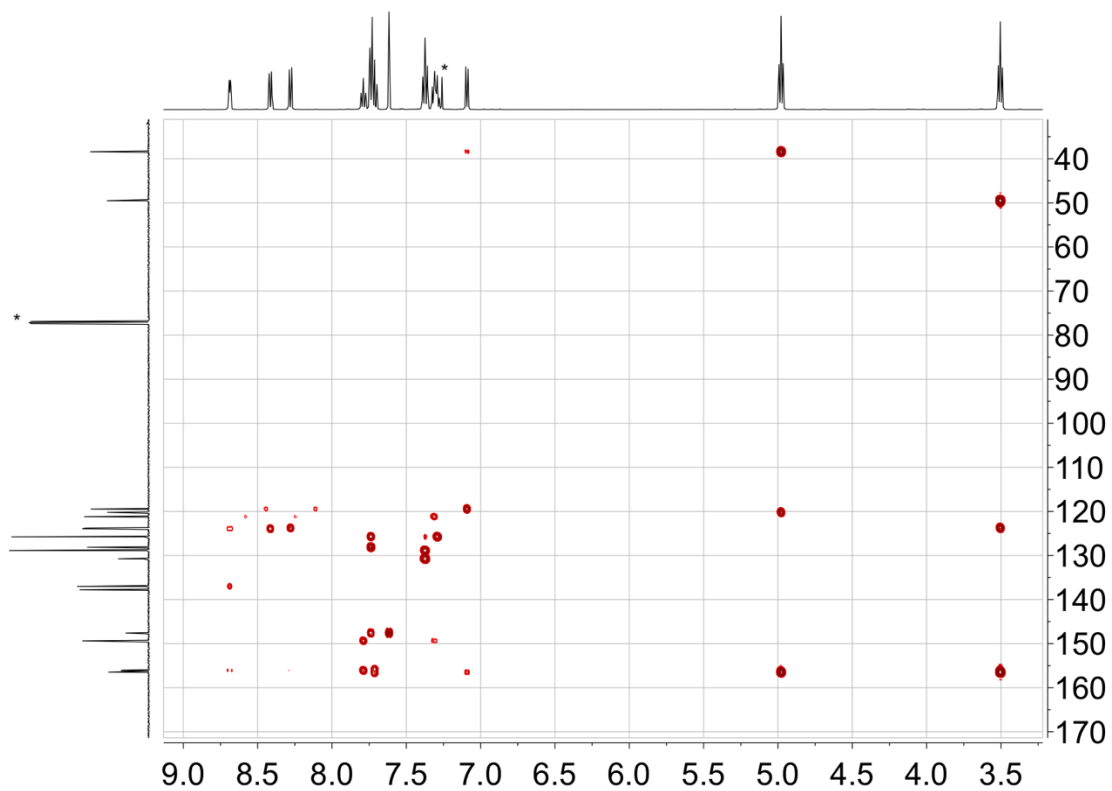


Figure S4. HMBC spectrum of **3** (^1H 500 MHz, ^{13}C 126 MHz, CDCl_3 , 298 K). * = CDCl_3 (in $^{13}\text{C}\{^1\text{H}\}$) or residual CHCl_3 (in ^1H); ** = H_2O .

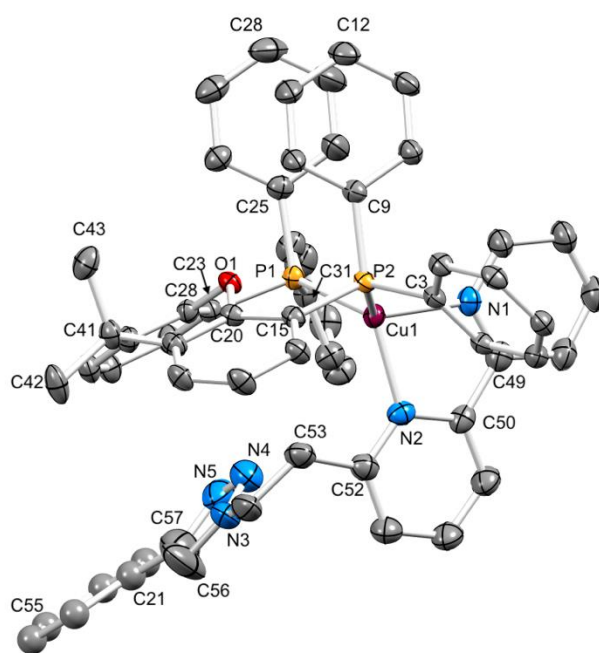


Figure S5. ORTEP representation of the structure of the $[\text{Cu}(\text{xantphos})(\mathbf{3})]^+$ cation in $[\text{Cu}(\text{xantphos})(\mathbf{3})][\text{PF}_6] \cdot 0.5\text{Et}_2\text{O}$. Ellipsoids are drawn at a 40% probability level and H atoms are omitted; the phenyl ring in ligand **3** was orientationally disordered and the rings were refined isotropically.

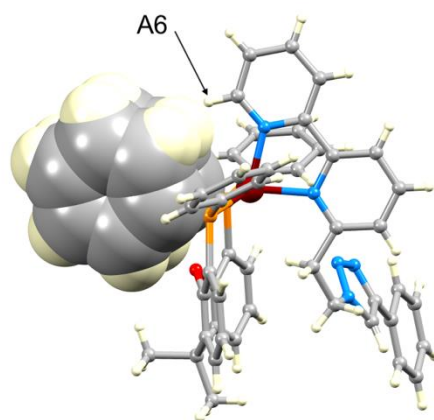


Figure S6. π -Stacking interaction in the $[\text{Cu}(\text{xantphos})(\mathbf{3})]^+$ cation and the proximity of proton H^{A6} to these phenyl rings.

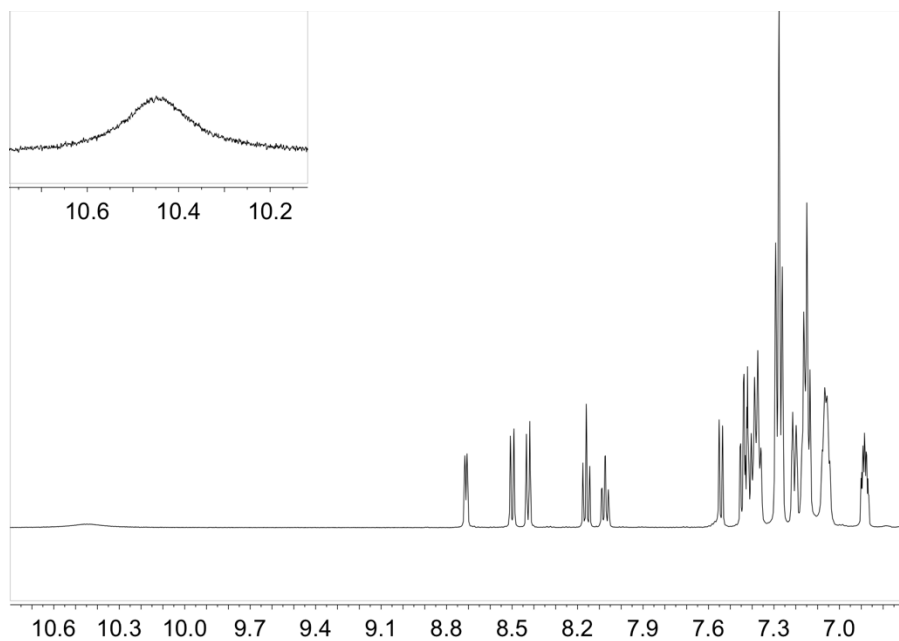


Figure S7. ^1H NMR spectrum of $[\text{Cu}(\text{POP})(\mathbf{1})][\text{PF}_6]$ (500 MHz, acetone- d_6 , 298 K) with the CO_2H signal inset.

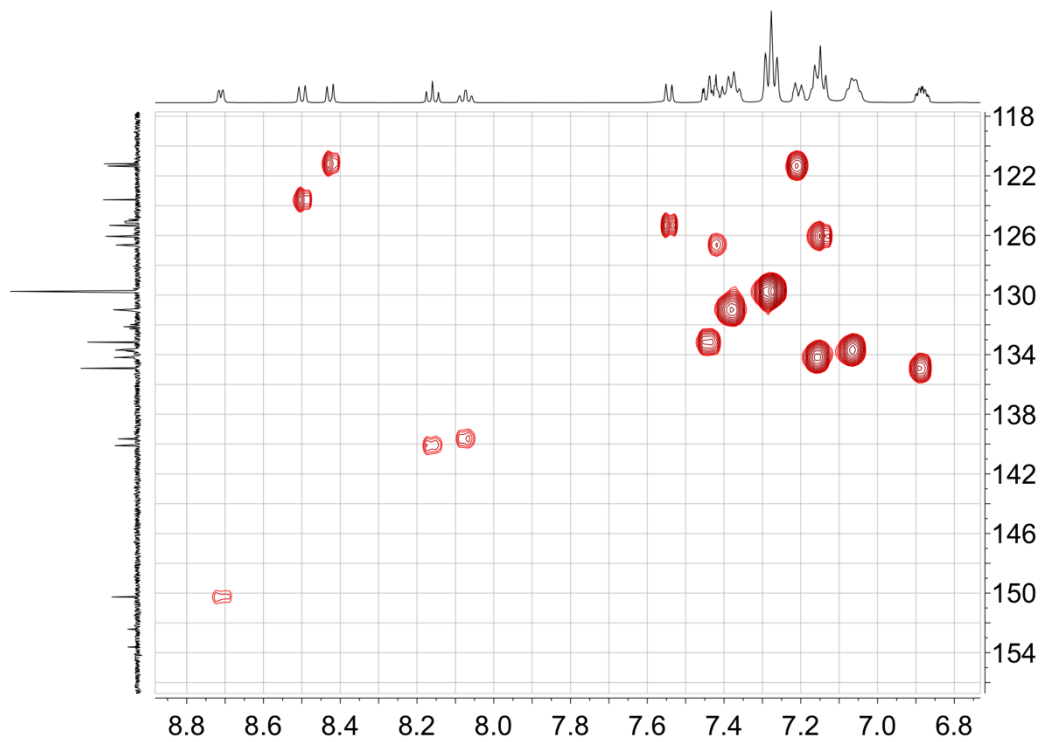


Figure S8. HMBC spectrum of $[\text{Cu}(\text{POP})(\mathbf{1})][\text{PF}_6]$ (^1H 500 MHz, ^{13}C 126 MHz, acetone- d_6 , 298 K).

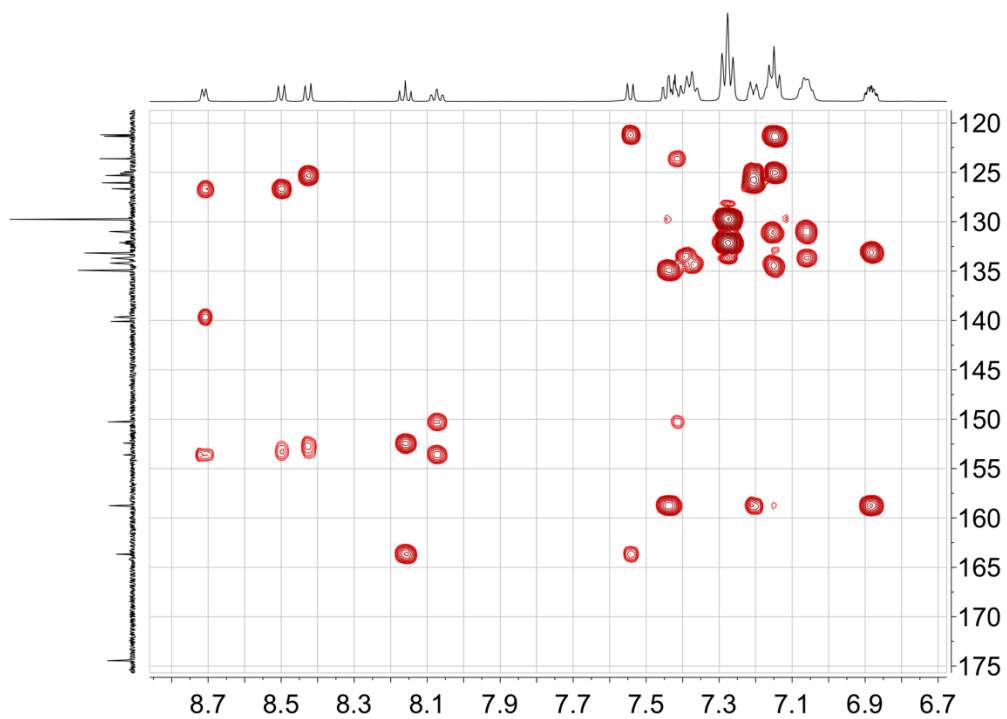


Figure S9. HMBC spectrum of $[\text{Cu}(\text{POP})(\mathbf{1})][\text{PF}_6]$ (^1H 500 MHz, ^{13}C 126 MHz, acetone- d_6 , 298 K).

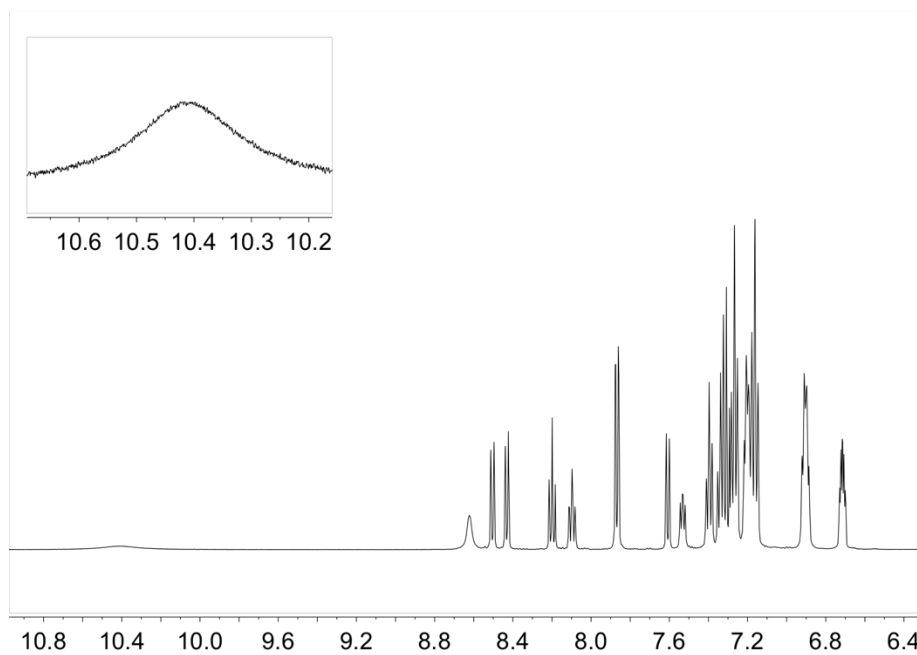


Figure S10. Part of the ^1H NMR spectrum of $[\text{Cu}(\text{xantphos})(\mathbf{1})][\text{PF}_6]$ (500 MHz, acetone- d_6 , 298 K) with the CO_2H signal inset.

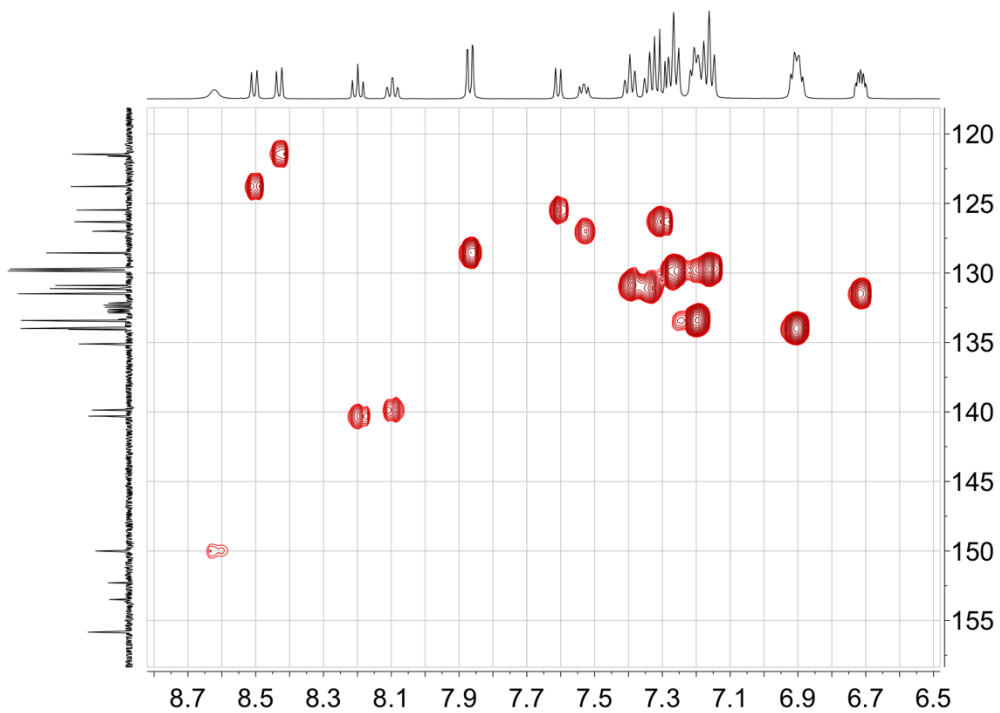


Figure S11. Part of the HMQC spectrum of [Cu(xantphos)(1)][PF₆] (¹H 500 MHz, ¹³C 126 MHz, acetone-d₆, 298 K).

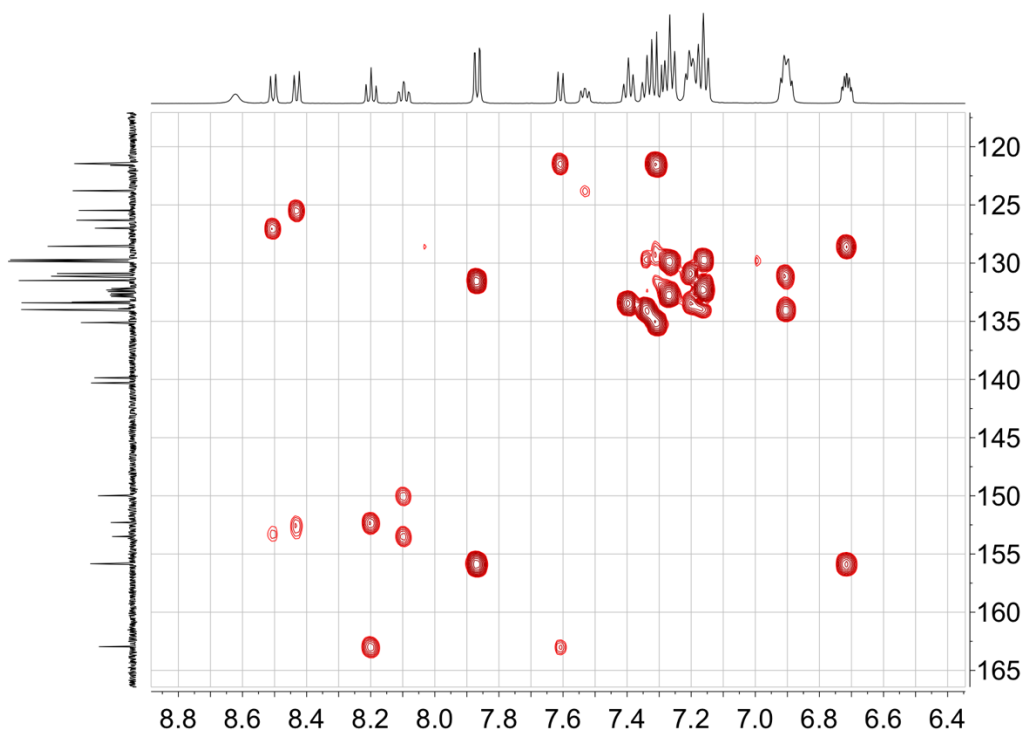


Figure S12. Part of the HMBC spectrum of [Cu(xantphos)(1)][PF₆] (¹H 500 MHz, ¹³C 126 MHz, acetone-d₆, 298 K).

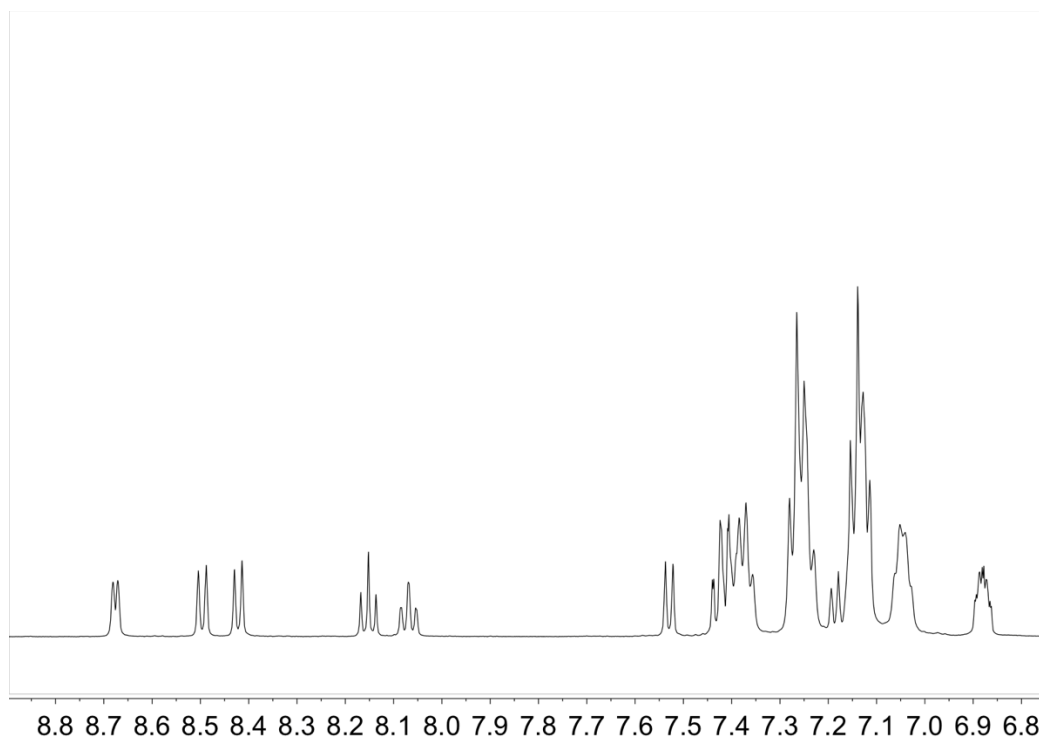


Figure S13. Aromatic region of the ^1H NMR spectrum of $[\text{Cu}(\text{POP})(\mathbf{2})][\text{PF}_6]$ (500 MHz, acetone- d_6 , 298 K).

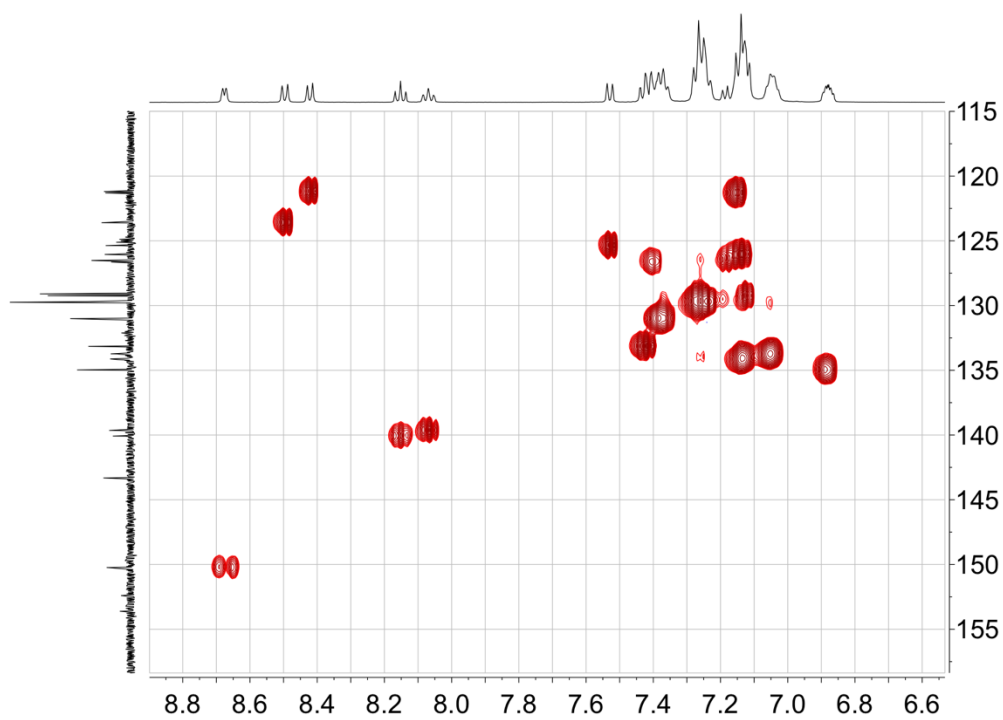


Figure S14. Aromatic region of the HMQC spectrum of $[\text{Cu}(\text{POP})(\mathbf{2})][\text{PF}_6]$ (^1H 500 MHz, ^{13}C 126 MHz, acetone- d_6 , 298 K).

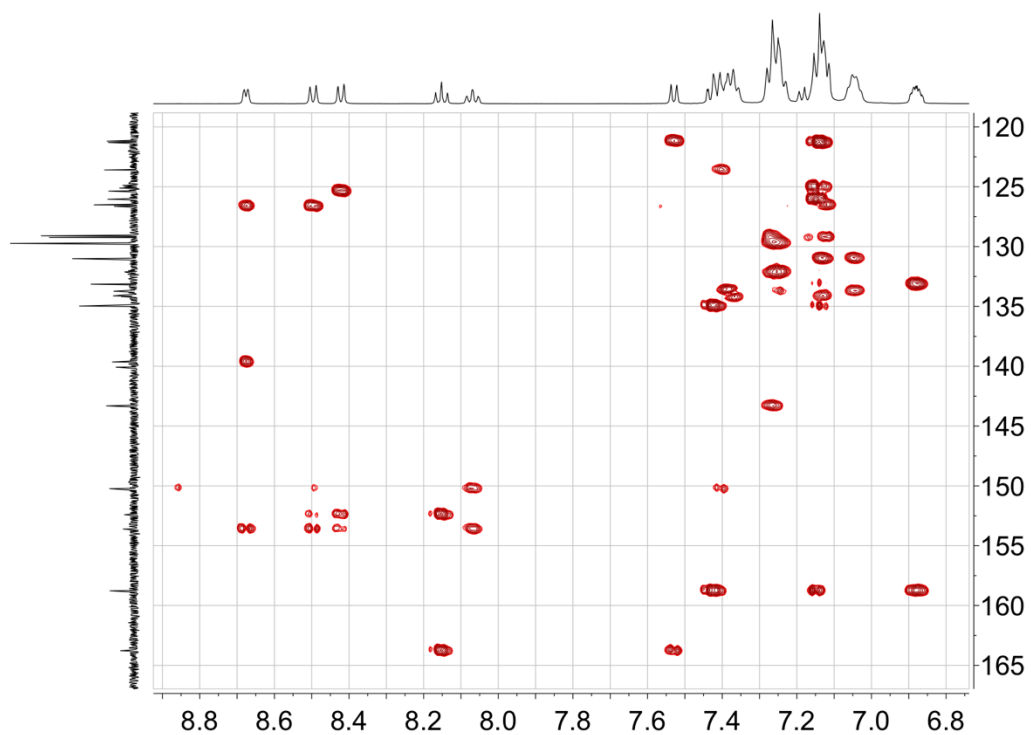


Figure S15. Aromatic region of the HMBC spectrum of $[\text{Cu}(\text{POP})(\mathbf{2})][\text{PF}_6]$ (^1H 500 MHz, ^{13}C 126 MHz, acetone- d_6 , 298 K).

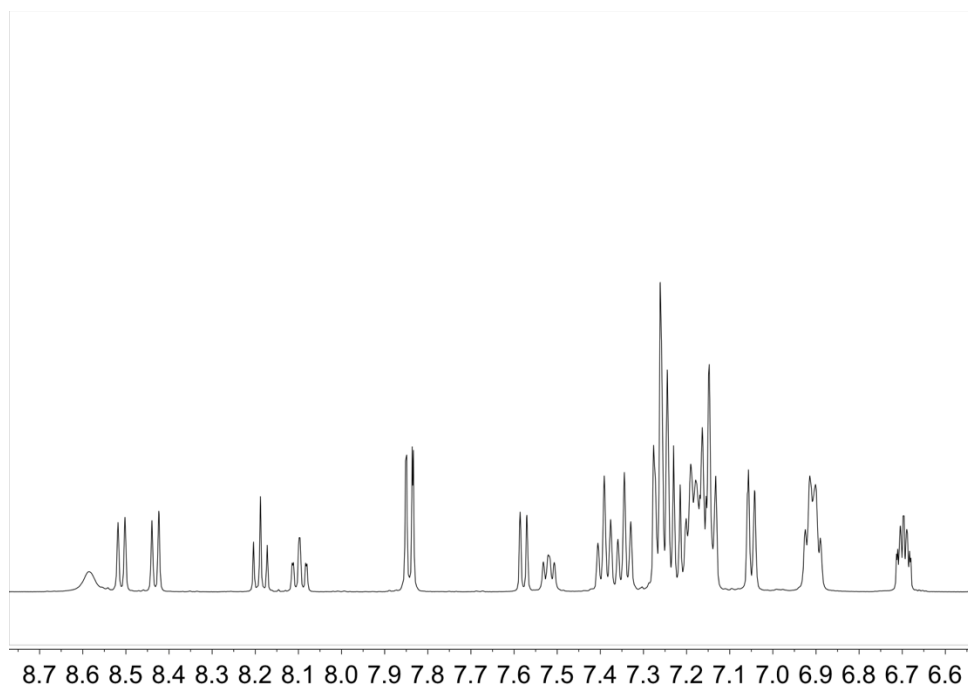


Figure S16. Aromatic region of the ^1H NMR spectrum of $[\text{Cu}(\text{xantphos})(\mathbf{2})][\text{PF}_6]$ (500 MHz, acetone- d_6 , 298 K).

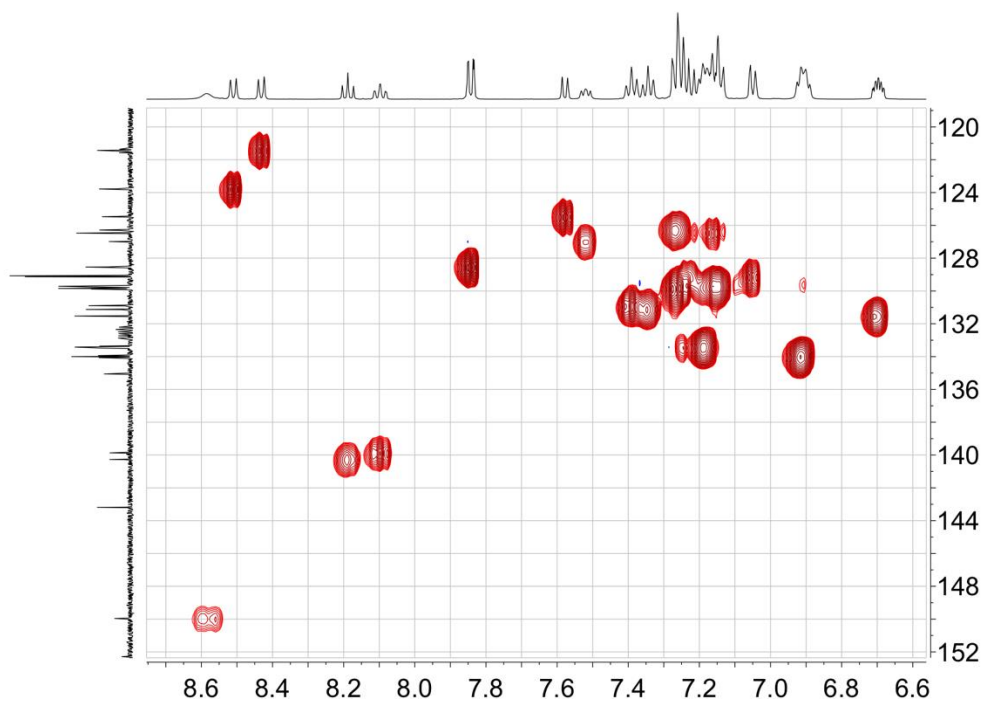


Figure S17. Aromatic region of the HMQC spectrum of $[\text{Cu}(\text{xantphos})(\mathbf{2})][\text{PF}_6]$ (^1H 500 MHz, ^{13}C 126 MHz, acetone- d_6 , 298 K).

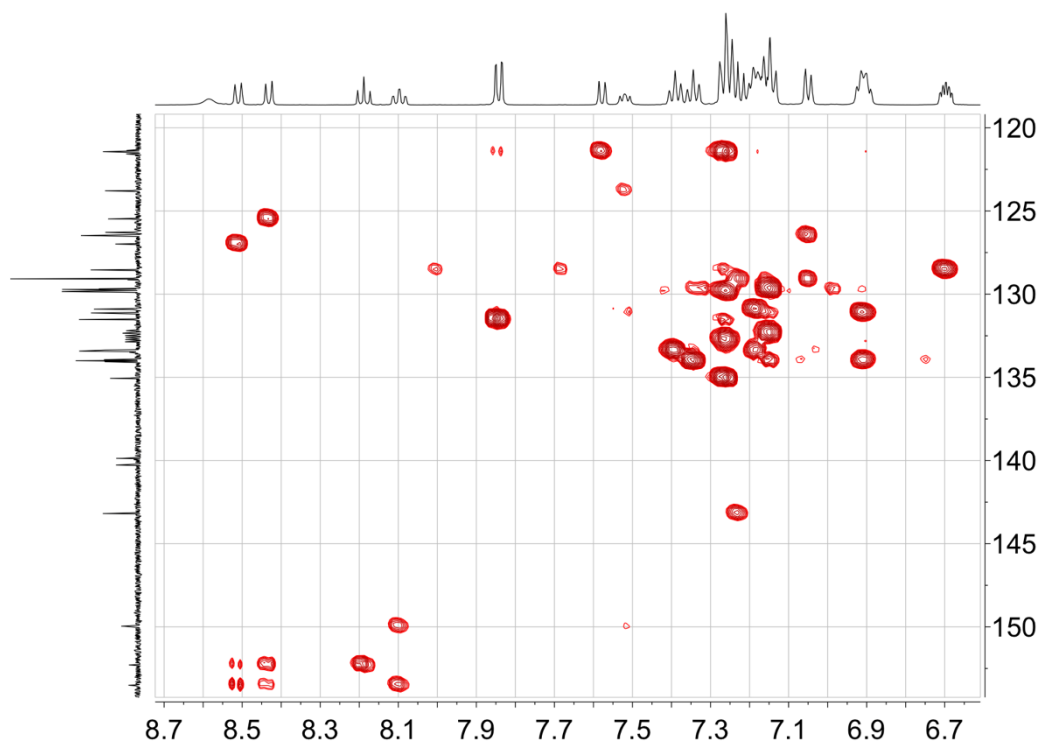


Figure S18. Aromatic region of the HMBC spectrum of $[\text{Cu}(\text{xantphos})(\mathbf{2})][\text{PF}_6]$ (^1H 500 MHz, ^{13}C 126 MHz, acetone- d_6 , 298 K).

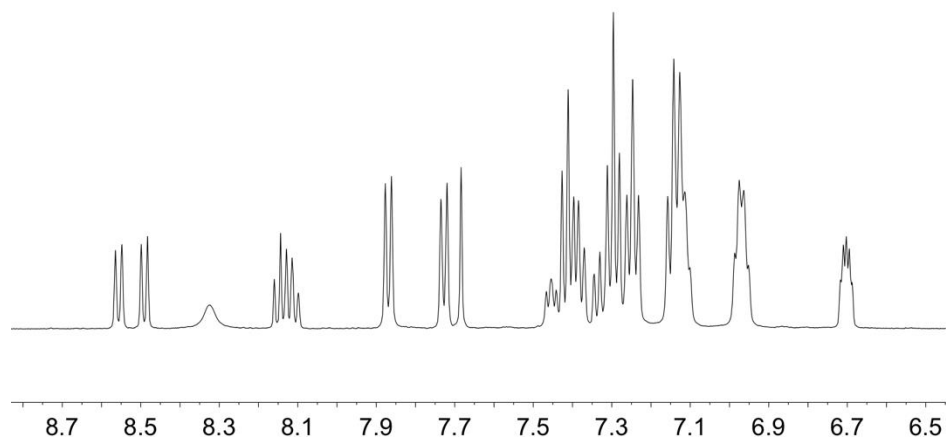


Figure S19. Aromatic region of the ^1H NMR spectrum of $[\text{Cu}(\text{xantphos})(\mathbf{3})][\text{PF}_6]$ (500 MHz, acetone- d_6 , 298 K).

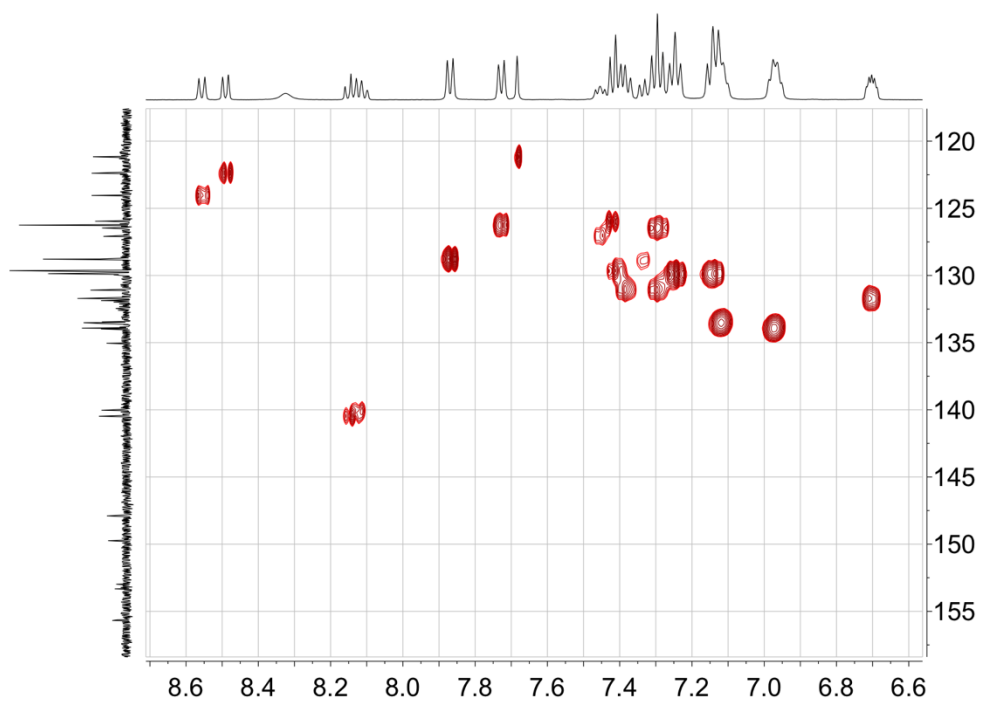


Figure S20. Aromatic region of the HMQC spectrum of $[\text{Cu}(\text{xantphos})(\mathbf{3})][\text{PF}_6]$ (^1H 500 MHz, ^{13}C 126 MHz, acetone- d_6 , 298 K).

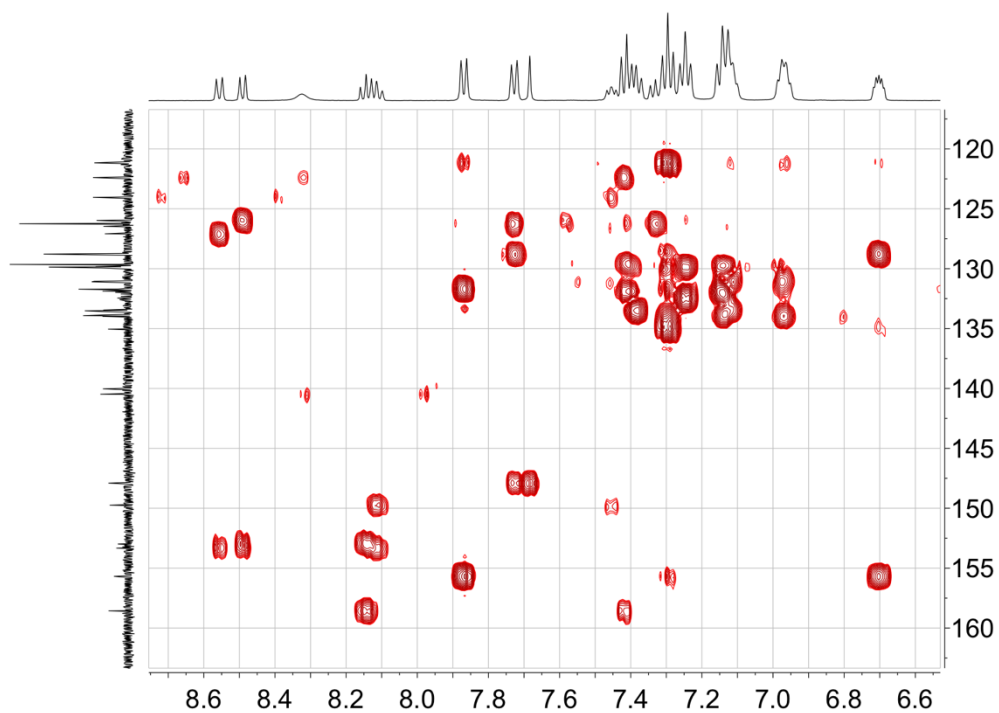


Figure S21. Aromatic region of the HMBC spectrum of $[\text{Cu}(\text{xantphos})(\mathbf{3})][\text{PF}_6]$ (^1H 500 MHz, ^{13}C 126 MHz, acetone- d_6 , 298 K).

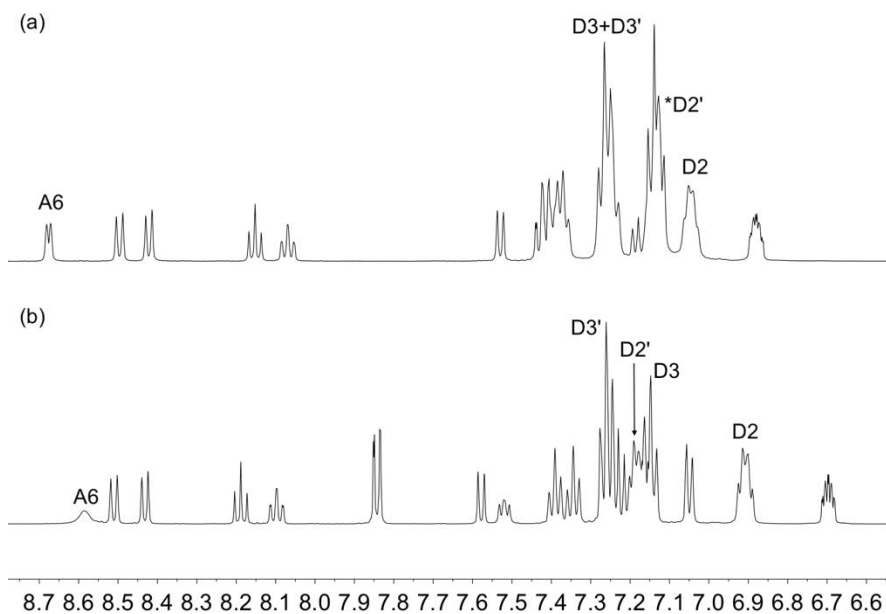


Figure S22. Aromatic regions of the ^1H NMR spectra (500 MHz, acetone- d_6 , 298 K) of (a) $[\text{Cu}(\text{POP})(\mathbf{2})][\text{PF}_6]$ and (b) $[\text{Cu}(\text{xantphos})(\mathbf{2})][\text{PF}_6]$. Compare with Figure 2 in the main article.

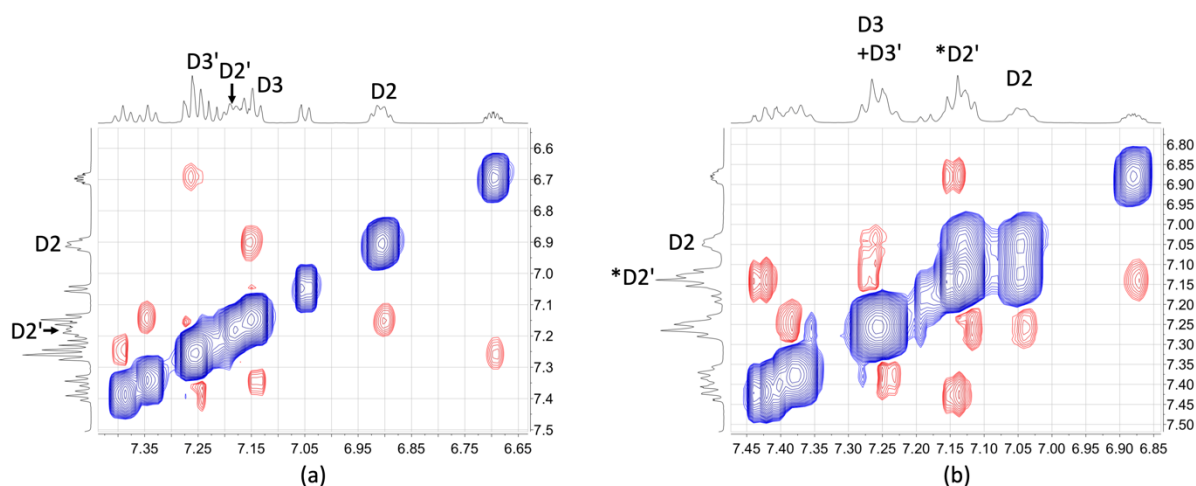


Figure S23. Part of the NOESY spectra (500 MHz, acetone-d₆, 298 K) of (a) [Cu(xantphos)(2)][PF₆] and (b) [Cu(POP)(2)][PF₆]. EXSY peaks appear in the opposite phase (blue) to NOESY crosspeaks (red), and are observed between H^{D2} and H^{D2'} in [Cu(POP)(2)][PF₆] but not in [Cu(xantphos)(2)][PF₆]. * The signal for D2' overlaps with signals assigned to E2, C4 and C6.

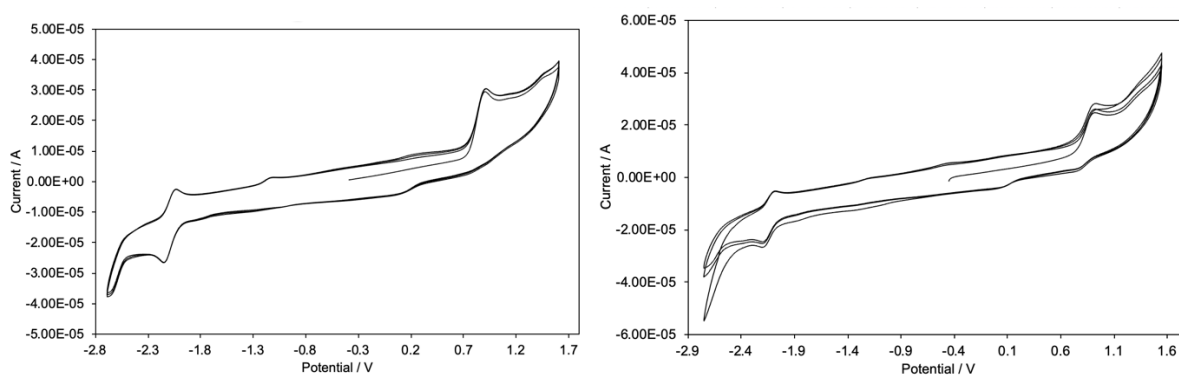


Figure S24. Three successive scans in the cyclic voltammograms of [Cu(POP)(2)][PF₆] (left) and [Cu(xantphos)(2)][PF₆] (right). Propylene carbonate solutions, and referenced internally to Fc/Fc⁺ = 0.0 V; [tBu₄N][PF₆] as supporting electrolyte and scan rate of 0.1 V s⁻¹.